Extract the Degradation Information in Squeezed States with Machine Learning

Hsien-Yi Hsieh, Yi-Ru Chen, Hsun-Chung Wu, Hua Li Chen, Jingyu Ning, Yao-Chin Huang, Chien-Ming Wu, and Ray-Kuang Lee

Phys. Rev. Lett. **128**, 073604 — Published 18 February 2022

DOI: 10.1103/PhysRevLett.128.073604

Extract the Degradation Information in Squeezed States with Machine Learning

Hsien-Yi Hsieh,[1] Yi-Ru Chen,[1] Hsun-Chung Wu,[1] Hua Li Chen,[2] Jingyu Ning,[1] Yao-Chin Huang,[1] Chien-Ming Wu,[1] and Ray-Kuang Lee[1,2,3,4]

[1]*Institute of Photonics Technologies, National Tsing Hua University, Hsinchu 30013, Taiwan*

[2]*Department of Physics, National Tsing Hua University, Hsinchu 30013, Taiwan*

[3]*Physics Division, National Center for Theoretical Sciences, Taipei 10617, Taiwan*

[4]*Center for Quantum Technology, Hsinchu 30013, Taiwan*[*]

(Dated: December 20, 2021)

Abstract

In order to leverage the full power of quantum noise squeezing with unavoidable decoherence, a complete understanding of the degradation in the purity of squeezed light is demanded. By implementing machine learning architecture with a convolutional neural network, we illustrate a fast, robust, and precise quantum state tomography for continuous variables, through the experimentally measured data generated from the balanced homodyne detectors. Compared with the maximum likelihood estimation method, which suffers from time-consuming and over-fitting problems, a well-trained machine fed with squeezed vacuum and squeezed thermal states can complete the task of reconstruction of the density matrix in less than one second. Moreover, the resulting fidelity remains as high as 0.99 even when the anti-squeezing level is higher than 20 dB. Compared with the phase noise and loss mechanisms coupled from the environment and surrounding vacuum, experimentally, the degradation information is unveiled with machine learning for low and high noisy scenarios, i.e., with the anti-squeezing levels at 12 dB and 18 dB, respectively. Our neural network enhanced quantum state tomography provides the metrics to give physical descriptions of every feature observed in the quantum state with a single-scan measurement just by varing the local oscillator phase from 0 to 2π and paves a way of exploring large-scale quantum systems in real-time.

Introduction.—With the intrinsic nature of multimode, continuous variable states have provided a powerful platform for generating large entangled networks [1–6]. In the family of continuous variables, *squeezed states*, even with the fundamental limit on the quantum fluctuations set by Heisenbergs uncertainty relation, remarkably exhibit completely different characteristics from discrete variables in the quantum world [7–9]. Now, as true applications, squeezed states have been used in quantum metrology [10–13], advanced gravitational wave detectors [14–20], generation of macroscopical states with a large photon number [21–23], and quantum information manipulation utilizing continuous variables [24, 25].

Even though up to 15 dB squeezing has been demonstrated as the state-of-the-art technology, any quantum system is unavoidably subject to a number of dissipative processes, causing 18-24 dB anti-squeezing accompanied [26]. Instead of dealing with pure states, the degradations in squeezing from loss and phase noise fluctuations limit the practical applications, resulting in tackling mixed states. The imperfection in purity is not only the obstacle for any quantum metrology with squeezed states, but also the restriction in generating larger-size Schrödinger's cat states. To access the non-classical power for quantum technologies, we need to have the ability to fully and precisely characterize the quantum features in a large Hilbert space. Utilizing multiple phase-sensitive measurements through homodyne detectors, quantum state tomography (QST) enables us to extract the complete information about the state of the system statistically [27, 28]. Nowadays, QST has been implemented in a variety of quantum systems, including quantum optics [29, 30], ultracold atoms [31, 32], ions [33, 34], and superconducting circuit-QED devices [35].

One of the most popular methods to implement QST is the maximum likelihood estimation (MLE) method, by estimating the closest probability distribution to the data for any arbitrary quantum states [36]. However, the required amount of measurements to reconstruct the quantum state in multiple bases increases exponentially with the number of involved modes. Albeit dealing with Gaussian quantum states, the MLE algorithm becomes computationally too heavy and intractable when the squeezing level increases. Moreover, MLE also suffers from the over-fitting problem when the number of bases grows. To make QST more accessible, several alternative algorithms are proposed by assuming some physical restrictions imposed upon the state in question, such as the permutationally invariant tomography [37], quantum compressed sensing [38], tensor networks [39, 40], and generative models [41]. Instead, with the capability to find the best fit to arbitrarily complicated data patterns with a limited number of parameters available, machine learning approaches are widely applied in many sub-fields in physics, from black hole detection, topological codes, phase transition, to quantum physics [42, 43]. For QST, the restricted Boltzmann machine has been applied to reduce the over-fitting problem in MLE [44].

In dealing with Gaussian states, methodologies based on covariance matrix or nullifiers are well-developed [45–47]. For the covariance method based on the homodyne measurements, at least three measurements must be performed at a fixed (but different) LO phase, in order to estimate the variances. Moreover, the assumption of pure squeezed part in the generated squeezed state is only valid for low squeezing levels. Nevertheless, information in different LO phases is missing due to the selected measurements only at three LO phases. When the squeezing level is higher than 5 dB, more and more non-pure squeezed parts become dominant, making these known methodologies inaccurate. Nowadays, higher than 10 dB squeezing levels are in the schedule for the advanced gravitational wave detectors [48, 49]. Even though for the non-ideal case, one can also apply the nullifiers to represent the actual noises in the operations by additional feedforward operations. A single-scan measurement to extract the degradation in quantum states is still missing.

Machine-learning QST.—Along this direction, based on the machine learning protocol, in particular with the convolutional neural network (CNN), we experimentally implement the quantum homodyne tomography for continuous variables and illustrate a fast, robust, and precise QST for

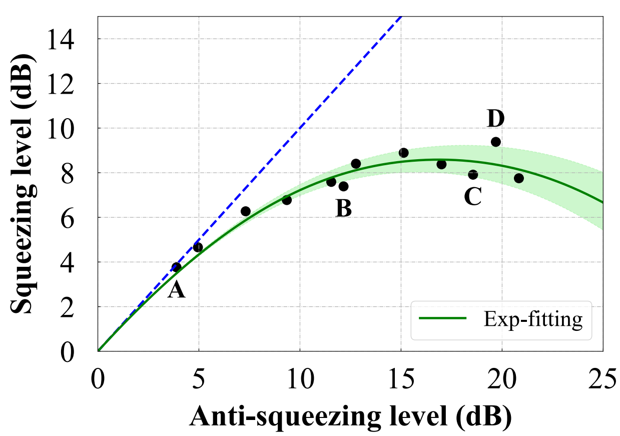

FIG. 1. Degradation in squeezed states. Ideally, the squeezing and anti-squeezing levels should locate along the Blue-dashed line. However, as shown with the typical experimental data, marked in Black dots, there exists a discrepancy between the measured squeezing and anti-squeezing levels. By taking the loss and phase noise into account, based on Eqs. (1-2), the optimal fitting curve is depicted in Green-color, with the corresponding standard deviation shown by the shadowed region.

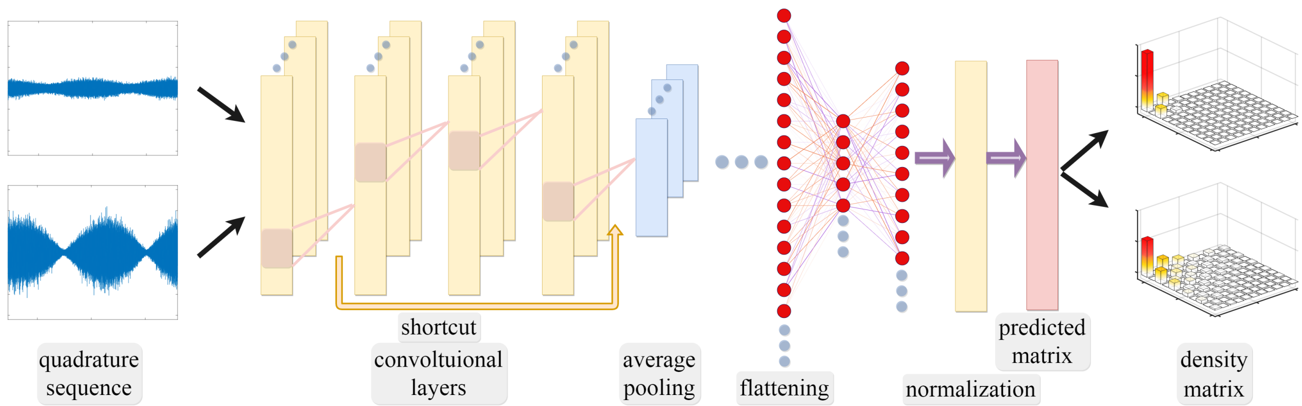

FIG. 2. Schematic of our precise and robust neural network enhanced quantum state tomography. The noisy data of quadrature sequence obtained by quantum homodyne tomography in a single-scan of LO phase from 0 to 2π, are fed to the convolutional layers, with the shortcut and average pooling in the architecture. Then, after flattening and normalization, the predicted matrices are inverted to reconstruct the density matrices in truncation.

squeezed states. As the time sequence data obtained in the optical homodyne measurements share the similarity to the voice (sound) pattern recognition, it motivates us to apply the CNN architecture. With the aim of realizing a fast QST, such a supervised CNN trained by the prior knowledge in squeezed states enables us to build a specific machine-learning for certain kinds of problems. More than two million data sets are fed into our machine with a variety of squeezed and thermal states in different squeezing levels, quadrature angles, and reservoir temperatures. When well-trained (typically in less than one hour), the execution time for our machine-learning enhanced QST takes the average cost time 38.1 milliseconds (by averaging 100 times) in a standard GPU server. Compared with the time-consuming MLE method, demonstrations on the reconstruction of the Wigner function and the corresponding density matrix are illustrated for squeezed vacuum states in less than one second (as 1 Hz scanning frequency is applied in a single-scan), keeping the fidelity up to 0.99 even taking 20 dB anti-squeezing level into consideration. Experimentally, the purity in squeezed vacuum states is evaluated directly for high squeezing levels (close to 10 dB squeezing level), but with low noisy and high noisy conditions, i.e., with the anti-squeezing levels at 12 dB and 18 dB, respectively. By extracting the purity of quantum states with the help of machine learning, a full understanding of the degradation in the state decoherence can also be unveiled in a single-scan measurement, paving the road toward a real-time QST to give physical descriptions of every feature observed in the quantum noise.

Experiments.—First of all, in Fig. 1, we show the degradation curve in typical squeezed state experiments, illustrated with the measured squeezing and anti-squeezing levels in the unit of decibel (dB). Here, our squeezed vacuum states are generated through a bow-tie optical parametric oscillator cavity with a periodically poled $KTiOPO_4$ (PPKTP) inside, operated below the threshold at the wavelength 1064 nm [50]. By injecting the AC signal of our homemade balanced homodyne detection, with the common-mode rejection ratio (CMRR) more than 80 dB, the spectrum analyzer records the squeezing and anti-squeezing levels by scanning the phase of the local oscillator. It is remarked that the value of CMRR not only tells how well the balanced signals from the two photodiodes can be suppressed, but also calibrates the measured values in squeezing levels [51]. Here, our measurements are collected by the spectrum analyzer at zero span mode. The phase of LO is scanned with a 1 Hz triangle wavefunction. Specifically, at 2.5 MHz, four experimental data are marked with the measured (squeezing:anti-squeezing) levels in dB: A (3.76: 3.89) at the pump power 5 mW, B (7.39:12.16) at 55 mW, C (7.91: 18.56) at 77 mW, and D (9.38:19.69) at 80 mW, respectively.

Ideally, without any degradation, the squeezing and anti-squeezing levels should be the same, located along the Blue-dashed line in Fig. 1. However, the phase noise and loss mechanisms coupled from the environment and surrounding vacuum set the limit on the measured squeezing level. These selected data represent nearly ideal squeezing (marker A), high squeezing level but with low degradation (marker B) and with high degradation (marker C); along with the highest squeezing level achieved (marker D with 9.38 dB in squeezing level).

By taking the optical loss (denoted as L) and phase noise (denoted as θ) into account, the measured squeezing V^{sq} and anti-squeezing V^{as} levels can be modeled as

$$V^{sq} = (1 - L)[V^{sq}_{id} \times \cos^2\theta + V^{as}_{id} \times \sin^2\theta] + L, \tag{1}$$

$$V^{as} = (1 - L)[V^{as}_{id} \times \cos^2\theta + V^{sq}_{id} \times \sin^2\theta] + L, \tag{2}$$

where V^{sq}_{id} and V^{as}_{id} are the squeezing and anti-squeezing levels in the ideal case. In Fig. 1, we also show the optimal fitting curve obtained by the orthogonal distance regression in Green-color, with the corresponding standard deviation (one-sigma variance) shown by the shadowed region.

Benchmarking of CNN-QST.—Even though by fitting several measured squeezing and anti-squeezing data one can estimate the degradation in squeezing empirically, the full information about the density matrix and the purity of quantum states needs to be reconstructed precisely

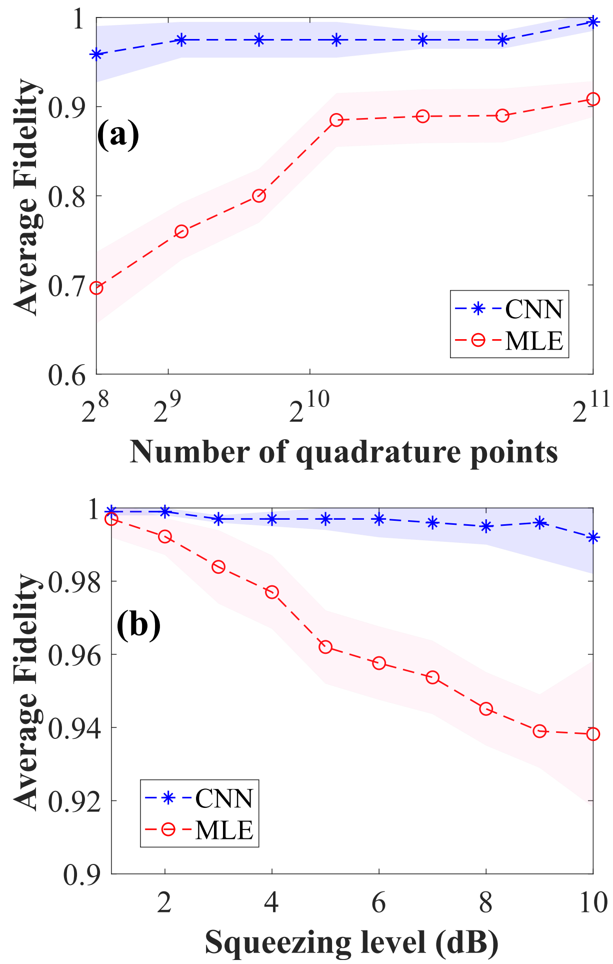

FIG. 3. Comparison in the average fidelity for the predicted density matrix obtained by maximum likelihood estimation (MLE) and convolution neural network (CNN) as a function of (a) the number of quadrature data points, and (b) the squeezing level. Here, $5,000$ simulated datasets are prepared for the comparison, but in (a) with different squeezing levels from 8 to 14 dB; while in (b), the number of data points in the quadrature sequence from 0 to 2π for the LO phase is fixed to $2,048$. The shadow regions represent the standard deviation in the average fidelity.

and fast. To generate QST for continuous variables, keeping the fidelity high and avoiding non-physical states are the critical issues in training our neural network enhanced tomography scheme. In training the reconstruction model, we use a *uniform distribution* to sample the value of LO angle, with $2,048$ sampling points fed from the experimental datasets ($5,000,000$ data points). As shown in Fig. 2, details about our machine learning architecture (including the hyper-parameters) and the reconstruction of the Wigner function, as well as the corresponding density matrix, are given in Supplemental Material.

To illustrate that our neural network enhanced QST indeed keeps the fidelity in the predicted density matrix, in Fig. 3, the average fidelity obtained by MLE and CNN are compared as a function of (a) the number of quadrature squence data points and (b) the squeezing levels (dB). Here, the fidelity is defined as $|\mathrm{tr}(\sqrt{\sqrt{\rho}\,\sigma\,\sqrt{\rho}})|^2$, with the given simulated input data ρ and the predicted density matrix σ obtained by MLE and CNN, respectively. The average is done with $5,000$ simulated datasets. As one can see in Fig. 3(a), when the number of quadrature points increases, from 256 to $2,048$, the resulting average fidelity increases even when we consider higher squeezing levels, i.e., 8 to 14 dB. Nevertheless, only with a small number of data points such as 256, the output fidelity obtained by CNN can be much higher than 0.95, compared to only 0.7 by MLE. Moreover, even the data point increases to $2,048$, MLE only gives the average fidelity up to 0.91, which is still much lower than 0.99 obtained by CNN.

On the other hand, when the data points are fixed to $2,048$, the superiority in CNN over MLE can also be clearly seen in Fig. 3(b), in particular at a higher squeezing level. Now, as the squeezing level increases, the dimension in the reconstructed Hilbert space exponentially grows. As a result, the average fidelity obtained by MLE decreases very quickly from 0.99 at a low (1 dB) squeezing level to 0.94 at a high (10 dB) squeezing level. On the contrary, our well-trained machine learning can keep the output fidelity as high as 0.99 even when 10 dB squeezing is tested.

Extracting the degradation information.—In addition to the reconstructed Wigner function and the corresponding density matrix, the degradation information in squeezing can be extracted directly from the predicted density matrix by calculating the purity of quantum state, i.e., $p \equiv \mathrm{tr}(\rho^2)$. The performance of our machine-learning QST is compared with the one obtained by the covariance matrix, denoted as the Exp-fitting curve in Fig. 4, as well as the one obtained by MLE, on the purity of squeezed states through the predicted density matrix. In addition to exhibiting the same trend in the degradation of purity, as one can see, at high squeezing levels, MLE over-estimates the purity of quantum states due to the over-fitting problem. On the contrary, the empirical formula under-estimates the purity due to the lack of thermal reservoir information.

Furthermore, we can directly apply the singular value decomposition to the predicted density matrix and extract the dominant terms, i.e., $\rho^{exp} = \sigma_1\,\rho^{sq} + \sigma_{non}\,\rho^{non}$, where $\sigma_{non}\,\rho^{non} = \sum_i c_i\,\rho^{sq}_{th,i} + \sum_i d_i\,\rho_{th,i}$ denotes the summation of all the contributed squeezed thermal states $\rho^{sq}_{th,i}$ and non-squeezed thermal states $\rho_{th,i}$, with the corresponding singular values c_i and d_i, respectively [54–56]. Here, the experimentally reconstructed density matrix ρ^{exp} is a mixed state but can

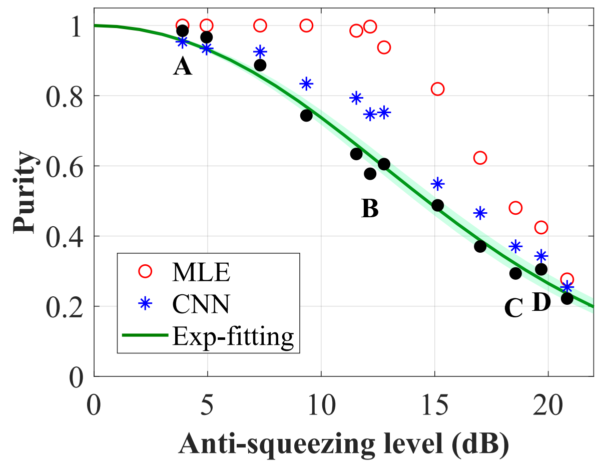

FIG. 4. The purity of squeezed states is plotted as a function of the measured anti-squeezing level. The experimental data marked in Fig. 1 are analyzed with MLE and CNN, plotted in Red- and Blue-colors, respectively. The fitting results based on Eqs. (1-2) are depicted in Green-curve, with the corresponding standard deviation shown in the shadow region. Here, at high squeezing levels, MLE over-estimates the purity of the quantum states in QST; while the empirical formula under-estimates the purity.

be decomposed to the incoherent sum of pure squeezed state ρ^{sq}, squeezed thermal states $\rho^{sq}_{th,i}$, and thermal states $\rho_{th,i}$. Note that there are many terms from the squeezed thermal states and thermal states. For the four selected experimental data, we have $\sigma_1 = 0.9764$, $\sigma_{non} = 0.0236$ for the nearly idea squeezing (marker A); $\sigma_1 = 0.8568$, $\sigma_{non} = 0.1432$ and $\sigma_1 = 0.7109$, $\sigma_{non} = 0.289$ for the high squeezing level but with low (marker B) and high (marker C) degradations, respectively. As for the highest squeezing level (markers D), we have $\sigma_1 = 0.5142$, $\sigma_{non} = 0.4858$.

To precisely identify the pure squeezed and noisy parts, in Fig. 5, with the help of machine learning, we can directly extract the three largest singular values corresponding to the coefficients in ideal (pure) squeezed state, the squeezed thermal state, and thermal state, i.e., $\rho^{\exp} = \sigma_1\, \rho^{sq} + c_1\, \rho^{sq}_{th} + d_1\, \rho_{th}$. Now, as shown in Fig. 5, it clearly illustrates that in addition to the pure squeezed states with the coefficient σ_1, there are two dominant terms in the degradation: from the contributions of thermal and squeezed thermal states. As expected, the thermal part, described by the coefficient d_1 in Blue-color, remains almost constant. It manifests the lossy effect due to the environment. It is a common belief that as long as the system is stable, the loss and phase noises can be measured by injecting classical laser light and be estimated. On the contrary, when the pump power increases, many additional effects, such as the heating in crystals,

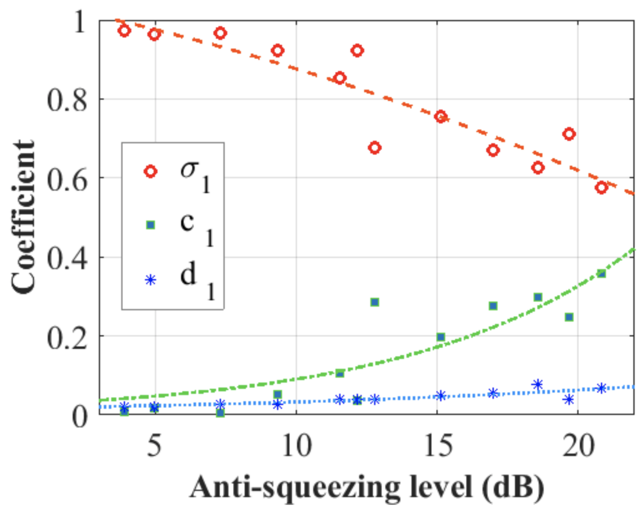

FIG. 5. With the help of machine learning, we can directly extract the degradation information from the obtained density matrix. Here, the three most significant singular values correspond to the coefficients in ideal (pure) squeezed state, the squeezed thermal state, and thermal state, i.e., $\rho = \sigma_1\,\rho^{sq} + c_1\,\rho^{sq}_{th} + d_1\,\rho_{th}$, respectively.

shift of resonance frequency, and/or other nonlinear mechanisms, occur, resulting in the increment in loss (see the Blue-color curve in our Fig. 5. Moreover, the other degradation effect from the squeezed thermal states, described by the coefficient c_1 in Green-color, increases as the (anti-) squeezing increases. It is this unexpected squeezed thermal state that causes severe degradation at higher squeezing levels [57, 58], which demonstrates the advantages of applying machine learning to QST. We want to remark that it is still unclear how to link the thermal states and/or squeezed thermal states to phase noise in a quantitative way. However, with this identification, one should be able to suppress and/or control the degradation at higher squeezing levels, which should be immediately applied to the applications for the gravitational wave detectors and quantum photonic computing.

Conclusion.—In conclusion, a neural network enhanced quantum state tomography is implemented experimentally for continuous variables. In particular, our well-trained machine fed with squeezed vacuum and squeezed thermal states not only completes the task of the reconstruction of the Wigner function in less than one second, but also keeps the high fidelity in the predict density matrix. Compared to the over-estimation by MLE and under-estimation by empirically fitting at high squeezing levels, the purity of squeezed states at squeezing level close to 10 dB is demonstrated experimentally, along with low and high anti-squeezing levels. Such a fast, robust, and precise quantum state tomography enables us to extract the degradation information in squeezing only with a single scan measurement. Our experimental implementations also act as the crucial diagnostic toolbox for the applications with squeezed states, including the advanced gravitational wave detectors, quantum metrology, macroscopic quantum state generation, and quantum information process.

Recently, taking advantages of this machine learning-based QST, not only the (static) Wigner distribution, but also the associated (dynamic) Wigner current are reconstructed experimentally [59]. In addition to the squeezed states illustrated here, similar concepts demonstrated in our well-trained machine can be readily applied to a specific family of continuous variables, such as non-Gaussian states. Of course, different training (learning) processes should be applied in dealing with single-photon states, Cat states, and GKP states. As illustrated in this work, a supervised machine-learning, such as the CNN used here, provides a good starting point for implementing QST with machine learning. In addition to CNN, with a better kernel developed in machine-learnings, it is possible to use less training data with a variety of machine learning architectures. For example, by applying the reinforce learning [60] or generative adversarial network (GAN) [61], quantum machine learning is expected to provide an efficient and robust way to explore the quantum world.

ACKNOWLEDGEMENT

We are indebted to the helps from Prof. Akira Furusawa, Prof. Ping Koy Lam and Dr. Syed Assad. This work is partially supported by the Ministry of Science and Technology of Taiwan (No. 108-2923-M-007-001-MY3 and No. 109-2112-M-007-019-MY3), Office of Naval Research Global, and the collaborative research program of the Institute for Cosmic Ray Research (ICRR), the University of Tokyo.

* rklee@ee.nthu.edu.tw

[1] S. L. Braunstein and P. van Loock, "Quantum information with continuous variables," Rev. Mod. Phys. **77**, 513 (2005).

[2] S. Yokoyama, R. Ukai, S. C. Armstrong, C. Sornphiphatphong, T. Kaji, S. Suzuki, J. Yoshikawa, H. Yonezawa, N. C. Menicucci, and A. Furusawa "Ultra-large-scale continuous-variable cluster states

multiplexed in the time domain," Nature Photonics **7**, 982-986 (2013).

[3] M. Chen, N. C. Menicucci, and O. Pfister, "Experimental Realization of Multipartite Entanglement of 60 Modes of a Quantum Optical Frequency Comb," Phys. Rev. Lett. **112**, 120505 (2014).

[4] J. Yoshikawa, S. Yokoyama, T. Kaji, C. Sornphiphatphong, Y. Shiozawa, K. Makino, and A. Furusawa, "Invited Article: Generation of one-million-mode continuous-variable cluster state by unlimited time-domain multiplexing featured," APL Photonics **1**, 060801 (2016).

[5] W. Asavanant, Y. Shiozawa, S. Yokoyama, B. Charoensombutamon, H. Emura, R. N. Alexander, S. Takeda, J. Yoshikawa, N. C. Menicucci, H. Yonezawa, and A. Furusawa, "Generation of time-domain-multiplexed two-dimensional cluster state," Science **366**, 373 (2019).

[6] M. V. Larsen, X. Guo, C. R. Breum, J. S. Neergaard-Nielsen, and U. L. Andersen, "Deterministic generation of a two-dimensionalcluster state," Science **366**, 369 (2019).

[7] H. P. Yuen, "Two-photon coherent states of the radiation field," Phys. Rev. A 1**3**, 2226 (1976).

[8] D. F. Walls and G. J. Milburn, *Quantum Optics*, 2nd Ed. (Springer, 1984).

[9] U. L. Andersen, T. Gehring, C. Marquardt, and G. Leuchs, "30 years of squeezed light generation," Phys. Scr. **91**, 053001 (2016).

[10] D. J. Wineland, J. J. Bollinger, W. M. Itano, F. L. Moore, and D. J. Heinzen, "Spin squeezing and reduced quantum noise in spectroscopy," Phys. Rev. A **46**, R6797 (1992).

[11] V. Giovannetti, S. Lloyd, and L. Maccone, "Quantum-enhanced measurements: beating the standard quantum limit," Science **306**, 1330 (2004).

[12] V. Giovannetti, S. Lloyd, and L. Maccone, "Advances in quantum metrology," Nature Photon. **5**, 222 (2011).

[13] S. Steinlechner, J. Bauchrowitz, M. Meinders, H. Muller-Ebhardt, K. Danzmann, and R. Schnabel, "Quantum-dense metrology," Nature Photon. **7**, 626 (2013).

[14] C. M. Caves, "Quantum-mechanical noise in an interferometer," Phys. Rev. D **23**, 1693 (1981).

[15] H. Grote, K. Danzmann, K. L. Dooley, R. Schnabel, J. Slutsky, and H. Vahlbruch, "First Long-Term Application of Squeezed States of Light in a Gravitational-Wave Observatory," Phys. Rev. Lett. **110**, 181101 (2013).

[16] L. Barsotti, J. Harms, and R. Schnabel, "Squeezed vacuum states of light for gravitational wave detectors," Rep. Prog. Phys. **82**, 016905 (2018).

[17] M. Tse et al., "Quantum-Enhanced Advanced LIGO Detectors in the Era of Gravitational-Wave Astronomy," Phys. Rev. Lett. **123**, 231107 (2019).

[18] F. Acernese et al. (Virgo Collaboration), "Increasing the Astrophysical Reach of the Advanced Virgo Detector via the Application of Squeezed Vacuum States of Light," Phys. Rev. Lett. 1**23**, 231108 (2019).

[19] Y. Zhao, N. Aritomi, E. Capocasa, M. Leonardi, M. Eisenmann, Y. Guo, E. Polini, A. Tomura, K. Arai, Y. Aso, Y.-C. Huang, R.-K. Lee, H. Luck, O. Miyakawa, P. Prat, A. Shoda, M. Tacca, R. Takahashi, H. Vahlbruch, M. Vardaro, C.-M. Wu, M. Barsuglia, and R. Flaminio, "Frequency-Dependent Squeezed Vacuum Source for Broadband Quantum Noise Reduction in Advanced Gravitational-Wave Detectors," Phys. Rev. Lett. **124**, 171101 (2020).

[20] L. McCuller, C. Whittle, D. Ganapathy, K. Komori, M. Tse, A. Fernandez-Galiana, L. Barsotti, P. Fritschel, M. MacInnis, F. Matichard, K. Mason, N. Mavalvala, R. Mittleman, H. Yu, M. E. Zucker, and M. Evans, "Frequency-Dependent Squeezing for Advanced LIGO," Phys. Rev. Lett. **124**, 171102 (2020).

[21] A. Ourjoumtsev, R. Tualle-Brouri, J. Laurat, and P. Grangier, "Generating Optical Schrodinger Kittens for Quantum Information Processing," Science **312**, 83 (2006).

[22] H. Takahashi, K. Wakui, S. Suzuki, M. Takeoka, K. Hayasaka, A. Furusawa, and M. Sasaki "Generation of Large-Amplitude Coherent-State Superposition via Ancilla-Assisted Photon Subtraction," Phys. Rev. Lett. 1**01**, 233605 (2008).

[23] D. V. Sychev, A. E. Ulanov, A. A. Pushkina, M. W. Richards, I. A. Fedorov, and A. I. Lvovsky, "Enlargement of optical Schrdinger's cat states," Nature Photonics **11**, 379 (2017).

[24] A. Furusawa, J. L. Sorensen, S. L. Braunstein, C. A. Fuchs, H. J. Kimble, and E. S. Polzik, "Unconditional Quantum Teleportation," Science **282**, 706 (1998).

[25] C. Weedbrook, S. Pirandola, R. Garca-Patrn, N. J. Cerf, T. C. Ralph, J. H. Shapiro, and S. Lloyd, "Gaussian quantum information," Rev. Mod. Phys. **84**, 621 (2012).

[26] H. Vahlbruch, M. Mehmet, K. Danzmann, and R. Schnabel, "Detection of 15 dB Squeezed States of Light and their Application for the Absolute Calibration of Photoelectric Quantum Efficiency," Phys. Rev. Lett. **117**, 110801 (2016).

[27] Z. Hradil, "Quantum-state estimation," Phys. Rev. A **55**, R1561(R) (1997).

[28] A. I. Lvovsky and M. G. Raymer, "Continuous-variable optical quantum-state tomography," Rev. Mod. Phys. **81**, 299 (2009).

[29] U. Leonhardt, *Measuring the Quantum State of Light*, (Cambridge University Press, 1997).

[30] U. L. Andersen, J. S. Neergaard-Nielsen, P. van Loock, and A. Furusawa, Hybrid discrete- and continuous-variable quantum information, Nature Phys. **11**, 713 (2015).

[31] D. Barredo, S. de Leseleuc, V. Lienhard, T. Lahaye, and A. Browaeys, “An atom-by-atom assembler of defect-free arbitrary two-dimensional atomic arrays,” Science 354, 1021 (2016).

[32] M. Endres, H. Bernien, A. Keesling, H. Levine, E. R. Anschuetz, A. Krajenbrink, C.Senko, V. Vuletic, M. Greiner, and M. D. Lukin, “Atom-by-atom assembly of defect-free one-dimensional cold atom arrays,” Science **354**, 1024 (2016).

[33] J. Zhang, G. Pagano, P. W. Hess, A. Kyprianidis, P. Becker, H. Kaplan, A. V. Gorshkov, Z.-X. Gong, and C. Monroe, “Observation of a many-body dynamical phase transition with a 53-qubit quantum simulator,” Nature **551**, 601 (2017).

[34] N. Friis, O. Marty, C. Maier, C. Hempel, M. Holzpfel, P. Jurcevic, M. B. Plenio, M. Huber, C. Roos, R. Blatt, and B. Lanyon, “Observation of entangled states of a fully controlled 20-qubit system,” Phys. Rev. X **8**, 021012 (2018).

[35] B. Vlastakis, G. Kirchmair, Z. Leghtas, S. E. Nigg, L. Frunzio, S. M. Girvin, M. Mirrahimi, M. H. Devoret, and R. J. Schoelkopf, “Deterministically encoding quantum information using 100- photon Schrodinger cat states,” Science **342**, 607 (2013).

[36] A. I. Lvovsky, “Iterative maximum-likelihood reconstruction in quantum homodyne tomography,” J. Opt. B: Quant. Semiclass. Opt. **6**, S556 (2004).

[37] G. Toth, W. Wieczorek, D. Gross, R. Krischek, C. Schwemmer, and H. Weinfurter, “Permutationally invariant quantum tomography,” Phys. Rev. Lett. **105**, 250403 (2010).

[38] D. Gross, Y.-K. Liu, S. T. Flammia, S. Becker, and J. Eisert, “Quantum state tomography via compressed sensing,” Phys. Rev. Lett. **105**, 150401 (2010).

[39] M. Cramer, M. B. Plenio, S. T. Flammia, D. Gross, S. D. Bartlett, R. Somma, O. Landon-Cardinal, D. Poulin, and Y.-K. Liu, “Efficient quantum state tomography,” Nature Commun. **1**, 149 (2010).

[40] B. P. Lanyon, C. Maier, M. Holzpfel, T. Baumgratz, C. Hempel, P. Jurcevic, I. Dhand, A. S. Buyskikh, A. J. Daley, M. Cramer, M. B. Plenio, R. Blatt, and C. F. Roos, “Efficient tomography of a quantum many-body system,” Nature Phys. **13**, 1158 (2017).

[41] J. Carrasquilla, G. Torlai, R. G. Melko, and L. Aolita, “Reconstructing quantum states with generative models,” Nature Mach. Intell. **1**, 155 (2019).

[42] J. Biamonte, P. Wittek, N. Pancotti, P. Rebentrost, N. Wiebe, and S. Lloyd, “Quantum machine learning,” Nature **549**, 195 (2017).

[43] S. Lohani, B. T. Kirby, M. Brodsky, O. Danaci, and R. T. Glasser, “Machine learning assisted quantum state estimation,” Mach. Learn.: Sci. Technol. **1**, 035007 (2020).

[44] E. S. Tiunov, V. V. Tiunova, A. E. Ulanov, A. I. Lvovsky, and A. K. Fedorov, “Experimental quantum homodyne tomography via machine learning,” Optica **7**, 448 (2020).

[45] P. Hyllus and J. Eisert, “Optimal entanglement witnesses for continuous-variable systems,” New J. Phys. **8**, 51 (2006).

[46] O. Pfister, “Continuous-variable quantum computing in the quantum optical frequency comb,” J. Phys. B: At. Mol. Opt. Phys. **53**, 012001 (2020).

[47] C. Fabre and N. Treps, ”Modes and states in quantum optics,” Rev. Mod. Phys. **92**, 035005 (2020).

[48] L. McCuller *et al.*, “LIGOs quantum response to squeezed states,” Phys. Rev. D **104**, 062006 (2021).

[49] C. Nguyen (for the Virgo Collaboration), “Status of the Advanced Virgo gravitational-wave detector,” arXiv: 2105.09247 (2021).

[50] C.-M. Wu, S.-R. Wu, Y.-R. Chen, H.-C. Wu, and R.-K. Lee, “Detection of 10dB vacuum noise squeezing at 1064 nm by balanced homodyne detectors with a common mode rejection ratio more than 80dB,” Conference on Lasers and Electro-Optics (CLEO), JTu2A.38 (2019).

[51] M. S. Stefszky, C. M. Mow-Lowry, S. S. Y. Chua, D. A. Shaddock, B. C. Buchler, H. Vahlbruch, A. Khalaidobski, R. Schnabel, P. K. Lam, and D. E. McClelland, “Balanced homodyne detection of optical quantum states at audioband frequencies and below,” Classical and Quantum Gravity **29**, 145015 (2012).

[52] A. Krizhevsky, I. Sutskever, and G. E. Hinton, “ImageNet classification with deep convolutional neural networks,” Comm. ACM. **60**, 84 (2017).

[53] K. He, X. Zhang, S. Ren, and Jian Sun, “Deep Residual Learning for Image Recognition,” Proc. IEEE Conf. Comp. Vision Pattern Recognition (CVPR), 770, (2016).

[54] G. S. Agarwal, “Wigner-function Description of Quantum Noise in Interferometers,” J. Mod. Opt. **34**, 909 (1987).

[55] S. Chaturvedi and V. Srinivasan, “Photon-number distributions for fields with Gaussian Wigner functions,” Phys. Rev. A **40**, 6095 (1989).

[56] N. Liitkenhaus and S. M. Barnett, “Nonclassical effects in phase space,” Phys. Rev. A **51**, 3340 (1995).

[57] M. J. Collett and C. W. Gardiner, “Squeezing of intracavity and traveling-wave light fields produced in parametric amplification,” Phys. Rev. A **30**, 1386 (1984).

[58] H.-C. Yuan and X.-X. Xu, "Squeezed vacuum state in lossy channel as a squeezed thermal state," Mod. Phys. Lett. **29**, 1550219 (2015).

[59] Y.-R. Chen, H.-Y. Hsieh, J. Ning, H.-C. Wu, H. L. Chen, Y.-L. Chuang, P. Yang, O. Steuernagel, C.-M. Wu, and R.-K. Lee, "Experimental Reconstruction of Wigner Distribution Currents in Quantum Phase Space," arXiv: 2111.08285 (2011).

[60] A. A. Melnikov, H. P. Nautrup, M. Krenn, V. Dunjkoa, M. Tiersch, A. Zeilinger, and H. J. Briegel, "Active learning machine learns to create new quantum experiments," Proc. Natl. Acad. Sci. USA **115**, 1221 (2018).

[61] S. Ahmed, C. S. Muoz, F. Nori, and A. F. Kockum, "Quantum State Tomography with Conditional Generative Adversarial Networks," Phys. Rev. Lett. **127**, 140502 (2021).